Optical Control of Cannabinoid Receptor 2–Mediated Ca^{2+} Release Enabled By Synthesis of Photoswitchable Probes

Roman C. Sarott,[†] Alexander E. G. Viray,[‡] Patrick Pfaff,[†] Anastasiia Sadybekov,[#] Gabriela Rajic,[‡] Vsevolod Katritch,[#] Erick M. Carreira,*[†] and James A. Frank*[‡]

[†] Laboratorium für Organische Chemie, Eidgenössische Technische Hochschule Zürich, Vladimir-Prelog-Weg 3, 8093 Zürich, Switzerland

[‡] Vollum Institute, Oregon Health & Science University, 3181 SW Sam Jackson Park Road, Portland, OR 97239-3098, USA

[#] Department of Biological Sciences and Department of Chemistry, Bridge Institute, University of Southern California, Los Angeles, California 90089, United States

KEYWORDS cannabinoids, cannabinoid receptor 2 (CB2), photopharmacology, Ca^{2+}-signaling, G protein-coupled receptor (GPCR)

ABSTRACT: Cannabinoid receptor 2 (CB2) is a promising target for the treatment of neuroinflammation and other diseases. However, lack of understanding of its complex signaling in cells and tissues complicates its therapeutic targeting. For the first time we show that HU308 increases cytosolic Ca^{2+} levels in mammalian cells *via* CB2 and phospholipase C. We report the synthesis of photoswitchable derivatives of CB2 agonist HU308, *azo*-HU308s, from central building block **3-OTf-HU308**. *Azo*-HU308s enable optical control over CB2 activity with spatiotemporal precision, as demonstrated in real-time Ca^{2+} fluorescence imaging. Our findings reveal a novel messenger pathway by which HU308 and its derivatives can affect cellular excitability, and demonstrate the utility of chemical photoswitches to control CB2 signaling in real time.

INTRODUCTION

The endocannabinoid system is a highly conserved lipid signaling system in all vertebrates, including humans, and is the subject of considerable research efforts aimed at its therapeutic exploitation.[1,2] It includes two classical cannabinoid receptors belonging to the class A family of G protein-coupled receptors (GPCRs).[3,4] Cannabinoid receptor 1 (CB1)[5] is highly expressed in the central nervous system and mediates the psychotropic effects of Δ^9-tetrahydrocannabinol (Δ^9-THC).[6–8] Cannabinoid receptor 2 (CB2)[9] is best known for its role in cells of the immune system.[8,10] Its expression and function in other cell types, tissues and organs remains highly contested. Pharmacological regulation of CB2 holds promise for the treatment of neurodegenerative diseases including Alzheimer's Disease, multiple sclerosis and amyotrophic lateral sclerosis, as well as tissue injury and inflammation.[1,11–14] Recently, several structures of CB2 have been elucidated by X-ray crystallography and electron microscopy, providing insight into CB2-ligand interactions.[15–17]

Functional understanding is required to fully realize the receptor's therapeutic potential. CB2 is linked to a large number of cellular signaling pathways[18] and exhibits pronounced biased signaling in response to different ligands and tissue-specific physiology.[19] Ca^{2+} ions are ubiquitous intracellular messengers in cellular signaling, and they are of emerging interest in connection with Alzheimer's and other neurodegenerative diseases linked to CB2.[20,21] Ca^{2+} is known to be released from a variety of extra- and intracellular reservoirs, which function at different timescales.[22–25] Surprisingly, CB2-mediated Ca^{2+} signaling remains poorly studied.[20–25] Deconvoluting the intricacies of these pathways requires the design of new functional chemical probes. For the highest degree of spatiotemporal control, light is the preferred stimulus. Photopharmacology, in which light is used for reversible isomerization of pharmacologically active ligands, has consequently emerged as a prominent approach allowing researchers to precisely manipulate signaling events in cells, tissues and organisms.[26,27] To this end, photopharmacological tools that enable dynamic control with spatial and temporal resolution over CB2-mediated Ca^{2+} signaling would open new avenues for the field.

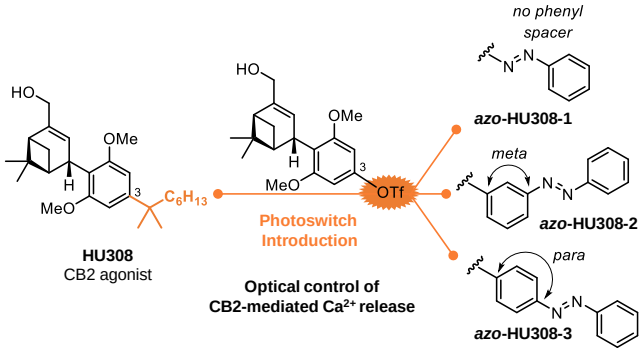

Figure 1. Photoswitchable *azo*-HU308 derivatives for optical control of CB2-mediated Ca^{2+} influx in mammalian cells.

We previously demonstrated for the first time reversible optical control over the endocannabinoid system.[28] Photoswitchable Δ^9-THC derivatives (*azo*-THCs) showed differential, light-dependent activity at CB1 receptors and activated multiple downstream CB1 effector pathways. *Azo*-THCs reversibly targeted CB1 to potentiate inwardly-rectifying K^+ channel currents and inhibit adenylyl cyclase activity. More recently, a report by Decker and co-workers described azobenzene-substituted benzimidazoles that displayed differential affinities towards CB2 in their *trans*- and *cis*-configurations.[29] However, no real-time control over CB2 signaling was demonstrated. As such, further studies to attain dynamic control, including the development of more advanced photoswitchable probes are required.

As a follow up to our work on CB1 optical control with Δ^9-THC derivatives, we examined ligands for CB2 inspired by HU308,[30] a commonly employed agonist. Interestingly, over the course of these studies we observed for the first time that HU308 stimulates intracellular Ca^{2+}-release in a mammalian cell line through CB2 and phospholipase C (PLC)-mediated pathways, which to the best of our knowledge has not been reported. We have leveraged these findings to devise photoswitchable HU308 azobenzene derivatives (*azo*-HU308s) which offer control over CB2-mediated Ca^{2+} release upon irradiation with light. This study presents a step forward in the biology of CB2, and highlights a novel effect of HU308 and its derivatives on CB2 effector pathways. Moreover, we utilize our findings to develop a CB2 assay based on fluorescent Ca^{2+} imaging, which is employed for the evaluation of *azo*-HU308s.

RESULTS

Design, synthesis, and characterization of photoswitchable HU308 derivatives

We based the design of photoswitchable ligands for CB2 on HU308, a benchmark CB2 agonist reported more than 20 years ago (Fig. 1).[30] It is a privileged ligand and widely used in CB2 pharmacology owing to its high affinity and potency.[19] Surprisingly, only recently it has been explored as blueprint for synthetic modification, leading to chemical tools for CB2. In this regard, replacement of the allylic alcohol in HU308 with an amide linkage enabled attachment of fluorescent dyes and led to highly specific probes.[31,32,] A wide range of substituents are tolerated at this position without affecting affinity as they extend out of the orthosteric binding pocket of CB2. By contrast, optical control over receptor activity requires identification of a different locus for photoswitch conjugation. In the ideal case, the resulting photopharmacological tools display differential activity in their respective light-induced configurations. Docking experiments suggested that the alkyl side chain of HU308 derivatives is embedded in the orthosteric binding pocket of CB2, and thus substitution at the 3'-position provides a starting point for our study (Fig. 1).[31,32]

Azobenzenes are the presently preferred switch in photopharmacology.[33] We devised three photoswitchable HU308 derivatives harboring azobenzenes. In ***azo*-HU308-1**, the phenyldiazene moiety is directly attached to the resorcinyl core, whereas ***azo*-HU308-2** and **-3** contain an additional phenyl spacer with *meta*/*para*-relationship between resorcinyl and diazene residues, respectively (Fig. 1). Importantly, we devised the synthesis based on common synthetic intermediate **3-OTf-HU308**, which facilitates late-stage azobenzene conjugation.

The synthesis of **3-OTf-HU308** commenced with the preparation of allylic alcohol **4** from (+)-verbenone (**1**), obtained in 62% yield by CrO_3-mediated oxidation of (+)-α-pinene. The use of *N*-hydroxyphthalimide as an additive proved critical to reduce oxidant loading and increase yield.[34] Treatment of **1** with Me_3SiOTf and *i*-Pr_2NEt afforded the corresponding silyl dienolether **2**, which without purification was subjected to epoxidation using *m*CPBA (Scheme 1).[35] Upon chromatographic purification on silica gel, γ-hydroxy verbenone **3** was obtained in 62% yield over 2 steps. This procedure for γ-oxidation proved more reliable and scalable than Wohl–Ziegler bromination followed by nucleophilic substitution.[31] TBS-protection of the primary alcohol and stereoselective 1,2-reduction of the enone by $NaBH_4$ afforded pinene-derived allylic alcohol **4** in high yield.[36] The central C-C bond of the HU308 scaffold was then installed by Friedel-Crafts allylation of phloroglucinol (**5**) with **4**, employing PPTS to give **6**.[37] The use of stoichiometric PPTS proved crucial for convenient reaction time and high yield of 85% as a single diastereomer.

Scheme 1. Synthesis of *azo*-HU308s

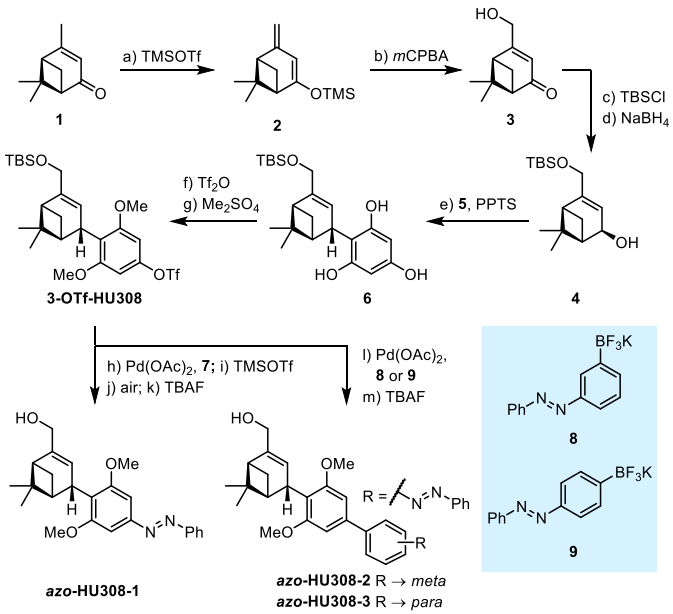

Reagents and conditions: a) Me_3SiOTf, DIPEA, CH_2Cl_2, 0 °C; b) *m*CPBA, AcOH, py, CH_2Cl_2, –25 °C, 62% over two steps; c) *t*-$BuMe_2SiCl$, NEt_3, DMAP, CH_2Cl_2, rt, 83%; d) $NaBH_4$, MeOH, rt, quantitative; e) phloroglucinol (**5**), PPTS, MeCN, rt, 85%; f) Tf_2O, 2,6-lutidine, CH_2Cl_2, rt, 66%; g) $(MeO)_2SO_2$, K_2CO_3, acetone, 40 °C, 93%; h) $Pd(OAc)_2$, $^tBu_3P{\cdot}HBF_4$, *N*-Boc-phenylhydrazine (**7**), Cs_2CO_3, toluene, 110 °C, 50%; i) Me_3SiOTf, 2,6-lutidine, CH_2Cl_2, 0 °C; j) $NaHCO_3$, MeOH, air, rt, 89% over two steps; k) Bu_4NF, THF, 0 °C to rt, 87%; l) $Pd(OAc)_2$, PCy_3, Cs_2CO_3, **8** or **9,** THF/water, 70 °C; m) Bu_4NF, THF, 0 °C to rt, 89% (*meta*), 94% (*para*) over two steps.

Phloroglucinol (**5**) as nucleophile prevented formation of undesired regioisomeric adduct, as observed for 3-bromoresorcinol.[38,39] Excess phloroglucinol (10 equiv) was required to suppress bis-allylations, which in turn necessitated MeCN as solvent to provide a homogeneous reaction mixture. Notably, this protocol circumvents the need for per-silylation of phloroglucinol as was reported by Makryannis and co-workers.[40,41] *Para*-selective phenol triflation (Tf_2O, 2,6-lutidine) and bis-*O*-methylation with $(MeO)_2SO_2$ afforded **3-OTf-HU308** in 61% yield over 2 steps. Finally, late stage derivatization was accomplished by means of cross-coupling chemistry. ***Azo*-HU308-1** was accessed using a sequence consisting of Buchwald–Hartwig coupling with *N*-Boc-phenylhydrazine (**7**), Boc-deprotection (Me_3SiOTf),[42] aerobic oxidation of the diaryl-hydrazine, and deprotection of TBS ether (38% yield over 4 steps). ***Azo*-HU308-2** and -**3** were prepared *via* cross-coupling with potassium trifluoroborate reagents[43,44] **8** and **9** under conditions reported by Molander and co-workers ($Pd(OAc)_2$, PCy_3, Cs_2CO_3, THF/water).[45] After TBS ether deprotection with Bu_4NF, ***azo*-HU308-2** and **-3** were obtained in excellent yields of 89 and 94% over 2 steps, respectively.

We proceeded to characterize the photophysical properties of *azo*-HU308s (Fig. 2). In their resting state, they reside in the thermodynamically favored *trans*-configuration. Illumination at 365 nm (UV-A) leads to a photostationary state (PSS) favoring the *cis*-isomer. Irradiation at 455 nm (blue light) leads to a new PSS with *trans* as the dominant isomer (Fig. 2, S1 and S2). *Trans*- and *cis*-isomer ratios at PSS were quantified by HPLC at the isosbestic wavelengths. At 365 nm, ***azo*-HU308-1-3** attain maximum *cis*-contents of 80, 71 and 49%, respectively.

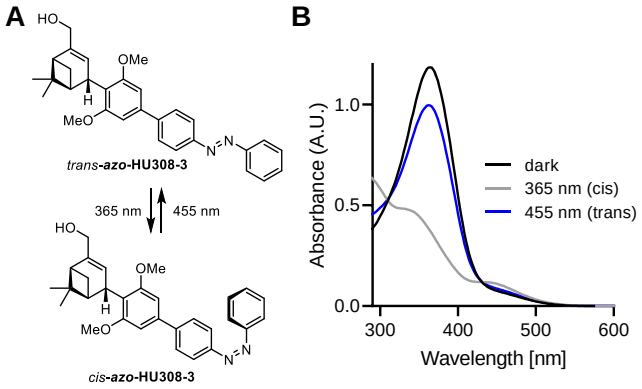

Figure 2. Photoisomerization of *azo*-HU308s. A) ***azo*-HU308-3** is isomerized between its *cis*- and *trans*-configurations with UV-A and blue irradiation, respectively. B) UV-Vis spectra of ***azo*-HU308-3** (50 μM in DMSO) in its dark-adapted (black), UV-A-adapted (grey,) and blue light-adapted (blue) photostationary states.

Subsequently, at 455 nm a new PSS is reached, with *trans*-contents of 83, 86 and 87% (Fig. S3 and S4). Additionally, *azo*-HU308s were bistable, with *cis*-***azo*-HU308-1-3** relaxing to their *trans*-isomers with thermal half-lives ($t_{1/2}$) of 4.7, 4.9 and 4.0 h in H_2Owater, respectively, as determined by the method of Priimagi and co-workers.[46]

Optical control of intracellular Ca2+ via CB2

A transformed mouse pituitary tumor AtT-20 cell line which stably expresses CB2 receptors (AtT-20(CB2) cells) reported by Mackie and co-workers was selected to explore the activity of our HU308-based photoswitches.[47] To confirm CB2 expression and membrane localization in this cell line, we utilized our recently reported HU308 derivative tagged with Alexa488 (Fig. S5A).[32] This non-permeable fluorescent probe binds specifically to CB2 receptors, and it allows receptor visualization in living cells using fluorescence microscopy. For comparison, both AtT-20(CB2) and AtT-20-wild-type cells lacking CB2[47,48] were incubated in parallel with fluoroprobe (150 nM, 10 min) and nuclear stain Hoechst33342 (20 μM, 10 min). In AtT-20(CB2) cells, Alexa488-fluorescence was observed on the outer plasma membrane of most cells (Fig. 3A,B, top, white arrows, Fig. S5B), confirming that CB2 is expressed on the cell surface. We did not observe plasma membrane fluorescence in AtT-20-wild-type cells (Fig. 3A,B, bottom, Fig. S5C), demonstrating the suitability of this fluorescent probe for specific visualization of CB2.

Classically, CB2 receptors are known to couple to $G\alpha_{i/o}$ proteins, which inhibit adenylyl cyclase activity and decrease cellular cyclic adenosine monophosphate (cAMP) concentrations.[16,49,50] More recent studies suggest that CB2 can also couple to other G proteins and effector pathways.[18,51,52] CB2 shows pronounced biased signaling on activation by different ligands, and the effects of CB2 activation on intracellular Ca^{2+} concentration ($[Ca^{2+}]_i$) have only been described on few occasions.[22,23,53–56] The study of $[Ca^{2+}]_i$ To the best of our knowledge, CB2-mediated modulation of $[Ca^{2+}]_i$ has not been reported for HU308 derivatives, thus we were intrigued to study Ca^{2+} signaling in living cells using HU308 and its photoswitchable derivatives. To assess the effect of HU308 in modulating CB2-mediated Ca^{2+} release, AtT-20(CB2) cells were loaded with Ca^{2+}-sensitive Fluo-4AM dye and subjected to fluorescent Ca^{2+} imaging (Fig. 3C, Fig. S6A).[57] Ionomycin (10 μM), which permeates cellular membranes, was added at the end of the experiment for normalization purposes. HU308 addition (20 μM) caused a large increase in Fluo-4 fluorescence intensity, indicating that CB2 activation causes an increase in $[Ca^{2+}]_i$ (Fig. 3C,D black). Irradiation at 375 nm (UV-A) did not affect $[Ca^{2+}]_i$ before or after HU308 addition, confirming that light alone does not affect $[Ca^{2+}]_i$ in AtT-20(CB2) cells, and that the effect of HU308 on $[Ca^{2+}]_i$ is not photosensitive. In control experiments, vehicle addition did not affect $[Ca^{2+}]_i$, both in presence and absence of irradiation (Fig. S6B,C).

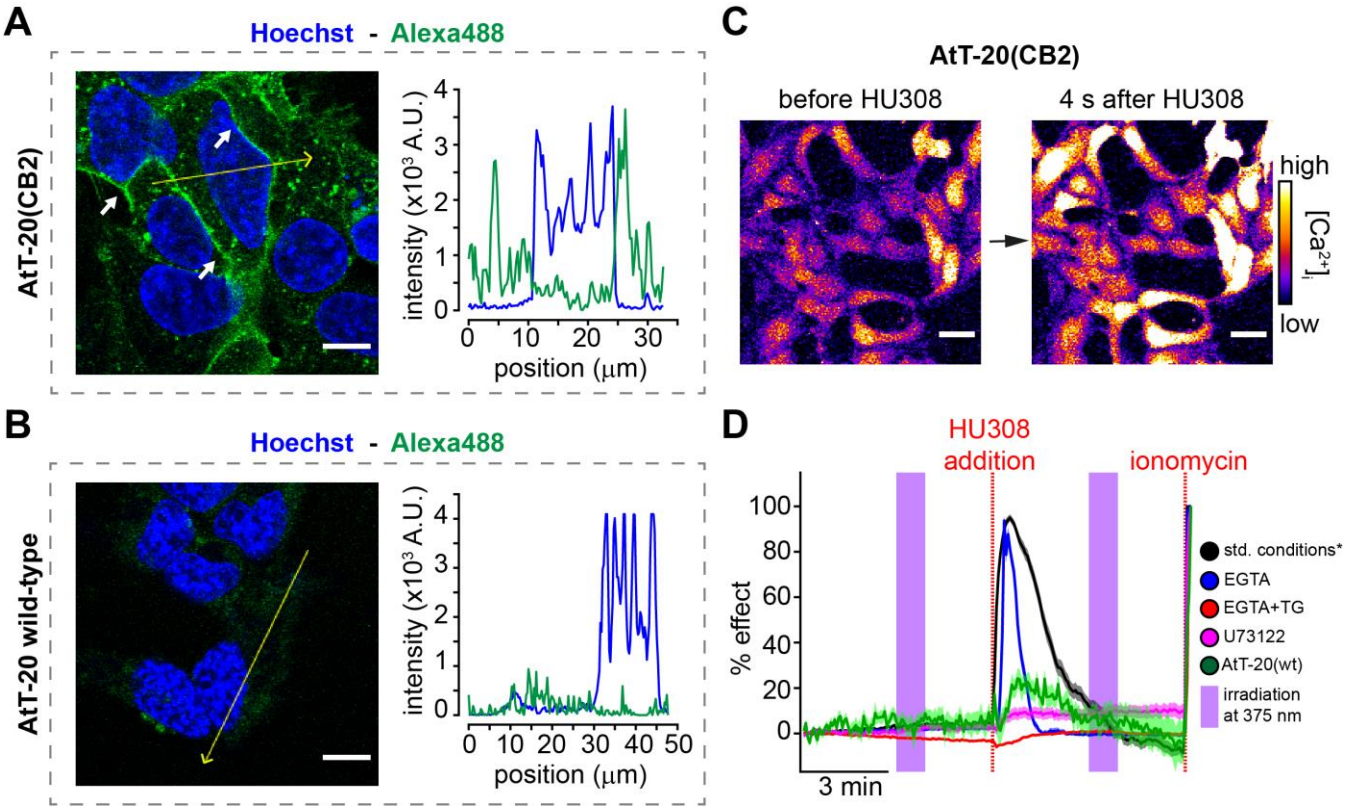

Figure 3. HU308 triggers Ca^{2+} influx in AtT-20(CB2) cells. (A,B) Fluorescent labeling of CB2 using Alexa488-tagged HU308 derivative in A) AtT-20(CB2) and B) AtT-20 wild-type cells. Nuclei were stained with Hoechst33342 and white arrows highlight CB2 plasma membrane localization Scale bars = 10 μm. *right panels* Intensity profile across the yellow line for Hoechst33342 and Alexa488 fluorescence. C) Representative Ca^{2+} images using Fluo-4 dye reveals addition of HU308 (20 μM) increases Ca^{2+} levels in AtT-20(CB2) cells. Scale bars = 30 μm. D) Average Fluo-4 intensity after addition of HU308 (20 μM) to AtT-20(CB2) cells in under standard conditions (black, buffer containing 1.2 mM $CaCl_2$), after sequestration of extracellular Ca^{2+} (blue, N = 100), addition of thapsigargin (TG, 5 μM, red, N = 100), or U73122 (10 μM, magenta, N = 99). The response to HU308 was sharply reduced wild-type cells (green, N = 100). Error bars = mean ±s.e.m.

Additionally, the effect of HU308 was substantially diminished in AtT-20-wild-type cells (Fig. 3D, green), confirming the involvement of CB2 in initiating the Ca^{2+} response. Cytososlic Ca^{2+} is kown to originate from both extracellular matrix as well as various intracellular reservoirs, including sarco/endoplasmic reticulum.[23] We thus sought to determine the mechanism by which HU308 and CB2 modulate $[Ca^{2+}]_i$ and to identify the source of Ca^{2+} ions observed. First, Ca^{2+} in the extracellular imaging buffer was sequestered by addition of chelator ethylene glycol-bis(2-aminoethylether)-*N,N,N',N'*-tetraacetic acid (EGTA, 0.1 mM), which prevents Ca^{2+} entry into the cell. Under these conditions HU308 addition caused a rise in $[Ca^{2+}]_i$ of approximately the same magnitude, however the effect subsided more rapidly when compared to experiments in the absence of EGTA (Fig. 3D, blue). Cells were then pretreated with thapsigargin (5 μM), a sarco/endoplasmic reticulum Ca^{2+}-ATPase (SERCA) pump blocker in presence of EGTA, to sequester extracellular Ca^{2+}. This combination completely abolished the effect of HU308 (Fig. 3D, red). Finally, addition of PLC inhibitor U73122 (10 μM)[58] greatly reduced the Ca^{2+} response induced by HU308 (Fig. 3D, pink). Taken together, these results indicate that HU308 stimulates Ca^{2+} release via CB2, $G\alpha_{q/11}$, and PLC. We surmise that this results in biphasic Ca^{2+} release from intracellular endo/sarcoplasmic reticulum Ca^{2+} stores, followed by activation of cell-surface Ca^{2+} channels. This coupling was previously demonstrated for the action of endocannabinoid 2-arachidonoyl glycerol (2-AG) at CB2.[23] However, to the best of our knowledge this represents a novel mechanism by which HU308 affects CB2 signaling at stimulatory GPCR effector pathways. We set out to explore the possibility of exerting optical control over CB2-mediated $[Ca^{2+}]_i$.

The three *azo*-HU308s were applied (each at 20 μM) to AtT20(CB2) cells loaded with Fluo-4AM dye, and their effects on $[Ca^{2+}]_i$ were recorded before and after photoswitching. In the case of ***azo*-HU308-1**, we observed a sharp increase in $[Ca^{2+}]_i$ on addition of the dark-adapted *trans*-configuration (Fig. 4C), and a ~23% decrease upon isomerization by irradiation at 375 nm. This suggests greater potency for ***azo*-HU308-1** in the *trans*-configuration. In contrast, ***azo*-HU308-2** shows no effect on $[Ca^{2+}]_i$ in either *trans*- or *cis*-form at this concentration (Fig. 4C). Most strikingly, ***azo*-HU308-3** did not affect $[Ca^{2+}]_i$ prior to irradiation but did lead to a sharp increase on irradiation at 375 nm, which suggests that only the *cis*-configuration has activity at CB2 (Fig. 4A). After termination of irradiation, the Ca^{2+} increase subsided. Similar to experiments involving HU308, addition of PLC inhibitor U73122 (10 μM) abolished the activity of ***azo*-HU308-3** in either *trans*- or *cis*-form (Fig. 4D, blue). Photoswitching was entirely absent in AtT-20-wild-type cells (Fig. 4D, black). These results confirm that ***azo*-HU308-3** signals through a mechanism identical to its parent compound, and demonstrates for the first time optical control over CB2-mediated Ca^{2+}-influx.

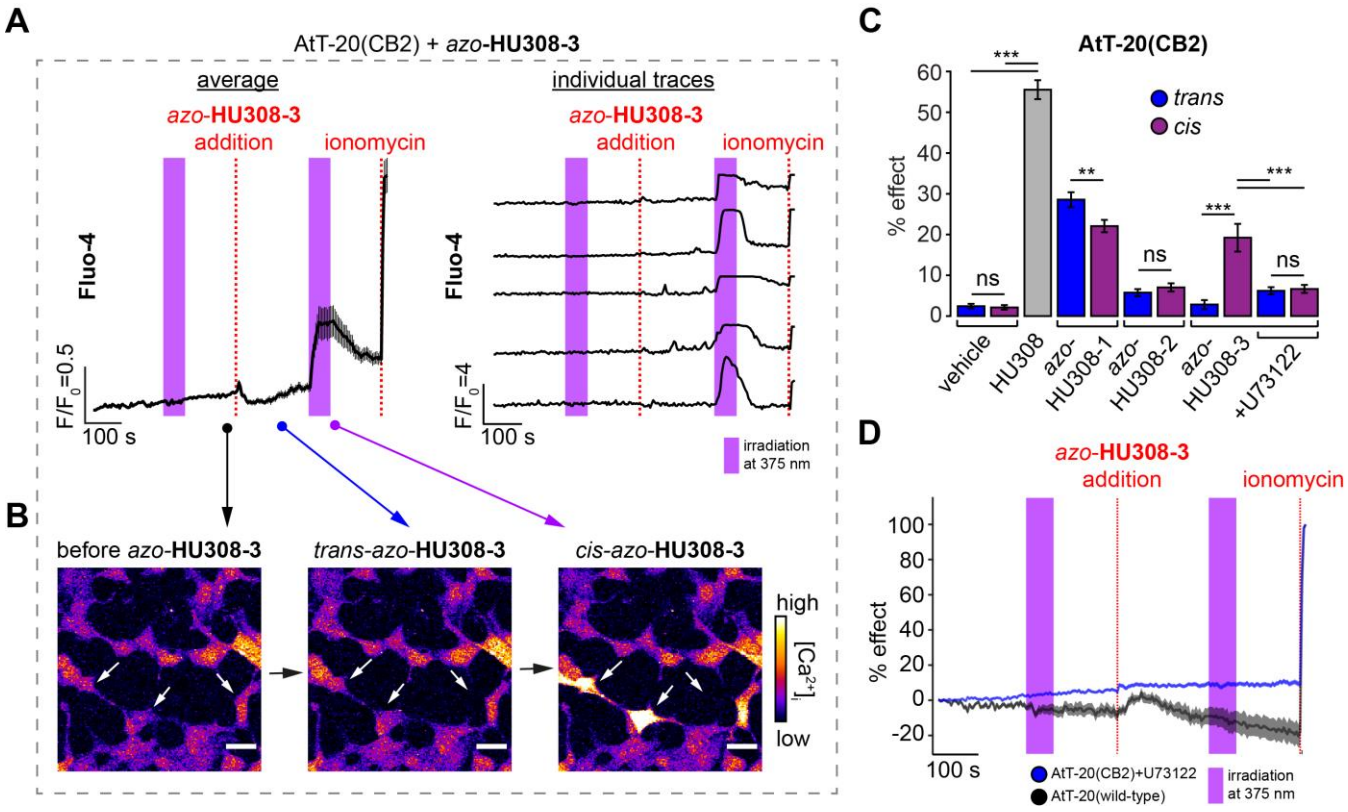

Figure 4. *Azo*-HU308s control Ca^{2+} influx in AtT-20(CB2) cells. A) Averaged (*left*) and single cell (*right*) Ca^{2+} imaging traces with Fluo-4 for ***azo*-HU308-3** (20 μM) showing an increase in Ca^{2+} induced by ***azo*-HU308-**3. Averaged data is displayed as average trace (65 technical, 2 biological replicates). B) Representative fluorescence images (scale bar = 30 μm) C) Summary bar graph for Ca^{2+} assay comparing vehicle (N = 80), HU308 (20 μM, N = 100), ***azo*-HU308-1** (20 μM, N = 150), ***azo*-HU308-2** (20 μM, N = 60), ***azo*-HU308-3** (20 μM, N = 65) and ***azo*-HU308-3** + U73112 (10 μM, N = 100) in *trans* (blue) and *cis* configuration (purple). D) Incubation with U73112 (blue, 10μM, N = 99) abolished the effect of ***azo*-HU308-3** (20 μM). AtT-20 wild-type cells did not respond to azo-HU308-3 (black, N = 99). Data averaged from 2 trials for each experiment. Error bars = mean ±s.e.m. *P<0.05, **P<0.01, ***P<0.001, ns = not significant.

Molecular Modelling and Docking

Flexible docking of HU308 and its azo-derivatives were performed with the structure of CB2 solved as co-crystal with agonist AM12033 (3.2 Å resolution).[16] To account for minor flexibility in the binding pocket, the conformations of receptor amino acid side chain within 8 Å radius from the ligands were co-optimized alongside ligand conformation. To establish the baseline values for prediction of ligand binding poses and scores, we performed redocking of co-crystallized agonist AM12033, as well as HU308 (Figure S7). The predicted docking pose of AM12033 showed strong agreement with the co-crystal structure (RMSD = 0.39Å) and high docking score (–35 kJ/mol). The pose of HU308 overlapped with AM12033 in the common parts of the scaffolds, and produced a comparable docking score (–30 kJ/mol).

Docking poses and scores were predicted for *cis*- and *trans*-isomers of each *azo*-HU308 (Table S1). The results show that all three active isomers, *trans*-***azo*-HU308-1**, *cis*-***azo*-HU308-1**, and *cis*-***azo*-HU308-3**, have docking scores of -27, -26 and -26 kJ/mol respectively. These are comparable to HU308, which is consistent with our experimental observations. The in silico binding poses for the resorcinyl-pinenyl core are similar to the predicted orientation of HU308. Their azobenzene moieties extend into the deep part of the hydrophobic binding pocket (Fig. 5). *Trans*-***azo*-HU308-3**, with its more extended configuration, failed to fit into the CB2 binding pocket, as it clashes with W2586.48. Both *trans*- and *cis*-***azo*-HU308-2** isomers docked with inferior binding scores (-13 and -16 kJ/mol, respectively), and with predicted poses that were dramatically distorted from that of HU308 (Fig. S8). This corroborates their lack of activity in our $[Ca^{2+}]_i$ assay. Interestingly, we observed that in order to accommodate the azobenzene substituent of some azo-HU308s, (e.g. *trans*-***azo*-HU308-1** and *cis*-***azo*-HU308-3**), the side chain of W2586.48 rotates about 30° without any substantial change in the surrounding residues (Fig. S9). This result suggests that the active state of CB2 has some flexibility in the orientation of W2586.48 side chain.

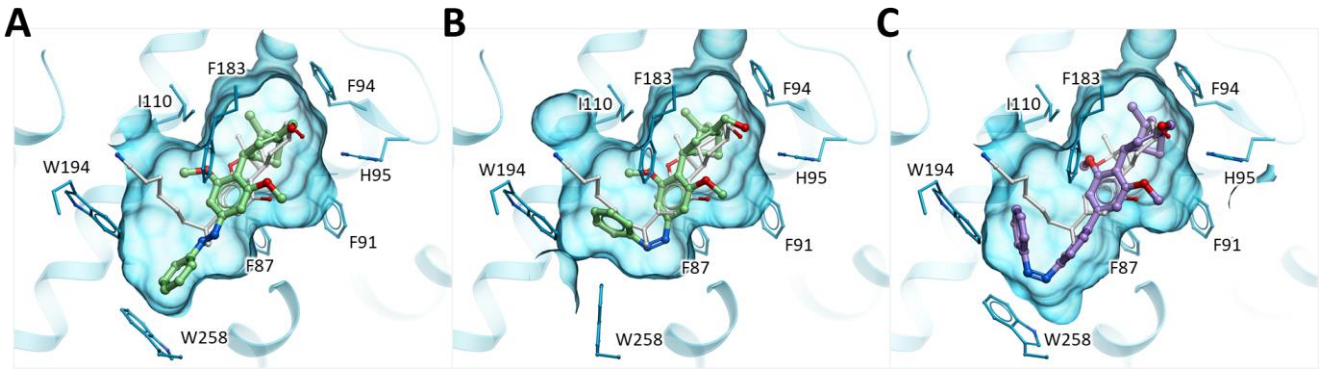

Figure 5. Predicted docking poses for A) *trans*-***azo*-HU308-1** B) *cis*-***azo*-HU308-1** and C) *cis*-***azo*-HU308-3**. *Trans*-***azo*-HU308-3** isomer is not shown as *cis*-to-*trans* switch results in major clashing with the receptor, which prevents reasonable docking. The CB2 co-crystal structure with agonist AM12033 (PDB ID: 6kpc) was used for docking. Receptor pocket is represented in blue sticks and transparent shape, and co-crystallized ligand AM12033 is shown in white. The predicted docking poses of ***azo*-HU308-1** are represented in green, and of ***azo*-HU308-3** in purple.

Conclusion

Synthesis of photoswitchable derivatives of HU308 led to two light-controllable probes for manipulating CB2 signaling. This was demonstrated by real-time Ca^{2+} imaging in mammalian cells. To the best our knowledge, our work represents the first observation of HU308 and its derivatives stimulating CB2/PLC-mediated Ca^{2+} influx in AtT-20(CB2) cells with high spatiotemporal precision. Importantly, the complementary (i.e. *trans*- vs. *cis*-active) behavior of ***azo*-HU308-1** and ***azo*-HU308-3** will be useful in designing experiments to manipulate CB2 in different physiological arenas. The experimental results were consistent with in silico docking studies into the CB2 binding pocket. In combination with the modular synthetic strategy, design of additional photoswitchable CB2 ligands with bespoke photophysical and pharmacological properties can be envisioned. For example, these may include red-shifted photochromic derivatives for use in intact tissue or in vivo.

A more detailed investigation into other downstream effector pathways controlled with *azo*-HU308s will provide insights on CB2 functional selectivity, which is crucial for understanding CB2 signaling across different cell types. In this regard, *azo*-HU308s have provided novel insights into the mechanisms by which CB2 affects cellular excitability. Application of *azo*-HU308s to more complex physiological settings will be useful for enhancing our understanding of CB2 in particular and of cannabinoid chemistry and biology in general.

AUTHOR INFORMATION

Corresponding Authors

*frankja@ohsu.edu

*erickm.carreira@org.chem.ethz.ch

Funding Sources

E.M.C. gratefully acknowledges support by ETH Zürich. R.C.S. and P.P. gratefully acknowledge funding from the Scholarship Fund of the Swiss Chemical Industry (SSCI). J.A.F., A.E.G.V., and G.R. acknowledge the Vollum Institute Fellowship for financial support.

Acknowledgement

We thank Ken Mackie for providing AtT-20 cell lines reagents and helpful discussions and Carsten Schultz for providing access to microscopy resources.

REFERENCES

(1) Pacher, P.; Kunos, G. Modulating the Endocannabinoid System in Human Health and Disease--Successes and Failures. *FEBS J.* **2013**, *280* (9), 1918–1943. https://doi.org/10.1111/febs.12260.

(2) Han, S.; Thatte, J.; Buzard, D. J.; Jones, R. M. Therapeutic Utility of Cannabinoid Receptor Type 2 (CB2) Selective Agonists. *J. Med. Chem.* **2013**, *56* (21), 8224–8256. https://doi.org/10.1021/jm4005626.

(3) Marzo, V. D.; Bifulco, M.; Petrocellis, L. D. The Endocannabinoid System and Its Therapeutic Exploitation. *Nature Reviews Drug Discovery* **2004**, *3* (9), 771–784. https://doi.org/10.1038/nrd1495.

(4) Maccarrone, M.; Bab, I.; Bíró, T.; Cabral, G. A.; Dey, S. K.; Di Marzo, V.; Konje, J. C.; Kunos, G.; Mechoulam, R.; Pacher, P.; Sharkey, K. A.; Zimmer, A. Endocannabinoid Signaling at the Periphery: 50 Years after THC. *Trends Pharmacol. Sci.* **2015**, *36* (5), 277–296. https://doi.org/10.1016/j.tips.2015.02.008.

(5) Matsuda, L. A.; Lolait, S. J.; Brownstein, M. J.; Young, A. C.; Bonner, T. I. Structure of a Cannabinoid Receptor and Functional Expression of the Cloned CDNA. *Nature* **1990**, *346* (6284), 561–564. https://doi.org/10.1038/346561a0.

(6) Gaoni, Y.; Mechoulam, R. Isolation, Structure, and Partial Synthesis of an Active Constituent of Hashish. *J. Am. Chem. Soc.* **1964**, *86* (8), 1646–1647. https://doi.org/10.1021/ja01062a046.

(7) Mechoulam, R. *Marijuana: Chemistry, Pharmacology, Metabolism and Clinical Effects*; Academic Press, 1973.

(8) Galiègue, S.; Mary, S.; Marchand, J.; Dussossoy, D.; Carrière, D.; Carayon, P.; Bouaboula, M.; Shire, D.; LE Fur, G.; Casellas, P. Expression of Central and Peripheral Cannabinoid Receptors in Human Immune Tissues and Leukocyte Subpopulations. *European Journal of Biochemistry* **1995**, *232* (1), 54–61. https://doi.org/10.1111/j.1432-1033.1995.tb20780.x.

(9) Munro, S.; Thomas, K. L.; Abu-Shaar, M. Molecular Characterization of a Peripheral Receptor for Cannabinoids. *Nature* **1993**, *365* (6441), 61–65. https://doi.org/10.1038/365061a0.

(10) Turcotte, C.; Blanchet, M.-R.; Laviolette, M.; Flamand, N. The CB2 Receptor and Its Role as a Regulator of Inflammation. *Cell. Mol. Life Sci.* **2016**, *73* (23), 4449–4470. https://doi.org/10.1007/s00018-016-2300-4.

(11) Guindon, J.; Hohmann, A. G. Cannabinoid CB2 Receptors: A Therapeutic Target for the Treatment of Inflammatory and Neuropathic Pain. *British Journal of Pharmacology* **2008**, *153* (2), 319–334. https://doi.org/10.1038/sj.bjp.0707531.

(12) Dhopeshwarkar, A.; Mackie, K. CB2 Cannabinoid Receptors as a Therapeutic Target—What Does the Future Hold? *Mol Pharmacol* **2014**, *86* (4), 430–437. https://doi.org/10.1124/mol.114.094649.

(13) Pacher, P.; Mechoulam, R. Is Lipid Signaling through Cannabinoid 2 Receptors Part of a Protective System? *Prg Lipid Res.* **2011**, *50* (2), 193–211. https://doi.org/10.1016/j.plipres.2011.01.001.

(14) Shoemaker, J. L.; Seely, K. A.; Reed, R. L.; Crow, J. P.; Prather, P. L. The CB2 Cannabinoid Agonist AM-1241 Prolongs Survival in a Transgenic Mouse Model of Amyotrophic Lateral Sclerosis When Initiated at Symptom Onset. *J. Neurochem.* **2007**, *101* (1), 87–98. https://doi.org/10.1111/j.1471-4159.2006.04346.x.

(15) Li, X.; Hua, T.; Vemuri, K.; Ho, J.-H.; Wu, Y.; Wu, L.; Popov, P.; Benchama, O.; Zvonok, N.; Locke, K.; Qu, L.; Han, G. W.; Iyer, M. R.; Cinar, R.; Coffey, N. J.; Wang, J.; Wu, M.; Katritch, V.; Zhao, S.; Kunos, G.; Bohn, L. M.; Makriyannis, A.; Stevens, R. C.; Liu, Z.-J. Crystal Structure of the Human Cannabinoid Receptor CB2. *Cell* **2019**, *176* (3), 459-467.e13. https://doi.org/10.1016/j.cell.2018.12.011.

(16) Hua, T.; Li, X.; Wu, L.; Iliopoulos-Tsoutsouvas, C.; Wang, Y.; Wu, M.; Shen, L.; Johnston, C. A.; Nikas, S. P.; Song, F.; Song, X.; Yuan, S.; Sun, Q.; Wu, Y.; Jiang, S.; Grim, T. W.; Benchama, O.; Stahl, E. L.; Zvonok, N.; Zhao, S.; Bohn, L. M.; Makriyannis, A.; Liu, Z.-J. Activation and Signaling Mechanism Revealed by Cannabinoid Receptor-Gi Complex Structures. *Cell* **2020**. https://doi.org/10.1016/j.cell.2020.01.008.

(17) Xing, C.; Zhuang, Y.; Xu, T.-H.; Feng, Z.; Zhou, X. E.; Chen, M.; Wang, L.; Meng, X.; Xue, Y.; Wang, J.; Liu, H.; McGuire, T. F.; Zhao, G.; Melcher, K.; Zhang, C.; Xu, H. E.; Xie, X.-Q. Cryo-EM Structure of the Human Cannabinoid Receptor CB2-Gi Signaling Complex. *Cell* **2020**. https://doi.org/10.1016/j.cell.2020.01.007.

(18) Saroz, Y.; Kho, D. T.; Glass, M.; Graham, E. S.; Grimsey, N. L. Cannabinoid Receptor 2 (CB2) Signals via G-Alpha-s and Induces IL-6 and IL-10 Cytokine Secretion in Human Primary Leukocytes. *ACS Pharmacol. Transl. Sci.* **2019**, *2* (6), 414–428. https://doi.org/10.1021/acsptsci.9b00049.

(19) Soethoudt, M.; Grether, U.; Fingerle, J.; Grim, T. W.; Fezza, F.; Petrocellis, L. de; Ullmer, C.; Rothenhäusler, B.; Perret, C.; Gils, N. van; Finlay, D.; MacDonald, C.; Chicca, A.; Gens, M. D.; Stuart, J.; Vries, H. de; Mastrangelo, N.; Xia, L.; Alachouzos, G.; Baggelaar, M. P.; Martella, A.; Mock, E. D.; Deng, H.; Heitman, L. H.; Connor, M.; Marzo, V. D.; Gertsch, J.; Lichtman, A.

H.; Maccarrone, M.; Pacher, P.; Glass, M.; Stelt, M. van der. Cannabinoid CB_2 Receptor Ligand Profiling Reveals Biased Signalling and off-Target Activity. *Nature Communications* **2017**, *8*, 13958. https://doi.org/10.1038/ncomms13958.
(20) Bezprozvanny, I. Calcium Signaling and Neurodegenerative Diseases. *Trends in Molecular Medicine* **2009**, *15* (3), 89–100. https://doi.org/10.1016/j.molmed.2009.01.001.
(21) LaFerla, F. M. Calcium Dyshomeostasis and Intracellular Signalling in Alzheimer's Disease. *Nature Reviews Neuroscience* **2002**, *3* (11), 862–872. https://doi.org/10.1038/nrn960.
(22) Zoratti, C.; Kipmen-Korgun, D.; Osibow, K.; Malli, R.; Graier, W. F. Anandamide Initiates Ca2+ Signaling via CB2 Receptor Linked to Phospholipase C in Calf Pulmonary Endothelial Cells. *Br J Pharmacol* **2003**, *140* (8), 1351–1362. https://doi.org/10.1038/sj.bjp.0705529.
(23) Brailoiu, G. C.; Deliu, E.; Marcu, J.; Hoffman, N. E.; Console-Bram, L.; Zhao, P.; Madesh, M.; Abood, M. E.; Brailoiu, E. Differential Activation of Intracellular versus Plasmalemmal CB2 Cannabinoid Receptors. *Biochemistry* **2014**, *53* (30), 4990–4999. https://doi.org/10.1021/bi500632a.
(24) Carafoli, E. Calcium Signaling: A Tale for All Seasons. *PNAS* **2002**, *99* (3), 1115–1122. https://doi.org/10.1073/pnas.032427999.
(25) Carafoli, E.; Krebs, J. Why Calcium? How Calcium Became the Best Communicator. *J. Biol. Chem.* **2016**, *291* (40), 20849–20857. https://doi.org/10.1074/jbc.R116.735894.
(26) Velema, W. A.; Szymanski, W.; Feringa, B. L. Photopharmacology: Beyond Proof of Principle. *J. Am. Chem. Soc.* **2014**, *136* (6), 2178–2191. https://doi.org/10.1021/ja413063e.
(27) Hüll, K.; Morstein, J.; Trauner, D. In Vivo Photopharmacology. *Chem. Rev.* **2018**. https://doi.org/10.1021/acs.chemrev.8b00037.
(28) Westphal, M. V.; Schafroth, M. A.; Sarott, R. C.; Imhof, M. A.; Bold, C. P.; Leippe, P.; Dhopeshwarkar, A.; Grandner, J. M.; Katritch, V.; Mackie, K.; Trauner, D.; Carreira, E. M.; Frank, J. A. Synthesis of Photoswitchable Δ9-Tetrahydrocannabinol Derivatives Enables Optical Control of Cannabinoid Receptor 1 Signaling. *J. Am. Chem. Soc.* **2017**, *139* (50), 18206–18212. https://doi.org/10.1021/jacs.7b06456.
(29) Dolles, D.; Strasser, A.; Wittmann, H.-J.; Marinelli, O.; Nabissi, M.; Pertwee, R. G.; Decker, M. The First Photochromic Affinity Switch for the Human Cannabinoid Receptor 2. *Adv. Therap.* n/a-n/a. https://doi.org/10.1002/adtp.201700032.
(30) Hanuš, L.; Breuer, A.; Tchilibon, S.; Shiloah, S.; Goldenberg, D.; Horowitz, M.; Pertwee, R. G.; Ross, R. A.; Mechoulam, R.; Fride, E. HU-308: A Specific Agonist for CB2, a Peripheral Cannabinoid Receptor. *Proc Natl Acad Sci U S A* **1999**, *96* (25), 14228–14233.
(31) Westphal, M. V.; Sarott, R. C.; Zirwes, E. A.; Osterwald, A.; Guba, W.; Ullmer, C.; Grether, U.; Carreira, E. M. Highly Selective, Amine-Derived Cannabinoid Receptor 2 Probes. *Chemistry – A European Journal* **2020**, *26* (6), 1380–1387. https://doi.org/10.1002/chem.201904584.
(32) Sarott, R.; Westphal, M.; Pfaff, P.; Korn, C.; Sykes, D.; Thais, G.; Brennecke, B.; Atz, K.; Weise, M.; Mostinski, Y.; Hompluem, P.; Eline, K.; Miljuš, T.; Roth, N.; Asmelash, H.; Vong, M.; Piovesan, J.; Guba, W.; Rufer, A. C.; A. Kusznir, E.; Huber, S.; Raposo, C.; Zirwes, E. A.; Osterwald, A.; Pavlovic, A.; Moes, S.; Beck, J.; Benito-Cuesta, I.; Grande, T.; Ruiz De Martin Esteban, S.; Yeliseev, A.; Drawnel, F.; Widmer, G.; Holzer, D.; Wel, T. van der; Mandhair, H.; Yuan, C.-Y.; Drobyski, W.; Saroz, Y.; Grimsey, N.; Honer, M.; Fingerle, J.; Gawrisch, K.; Romero, J.; Hillard, C. J.; Varga, Z. V.; Stelt, M. van der; Pacher, P.; Gertsch, J.; McCormick, P.; Ullmer, C.; Oddi, S.; Maccarrone, M.; Veprintsev, D. B.; Nazare, M.; Grether, U.; Carreira, E. Development of High-Specificity Fluorescent Probes to Enable Cannabinoid Type 2 Receptor Studies in Living Cells. **2020**. https://doi.org/10.26434/chemrxiv.12356597.v1.
(33) Broichhagen, J.; Frank, J. A.; Trauner, D. A Roadmap to Success in Photopharmacology. *Acc. Chem. Res.* **2015**, *48* (7), 1947–1960. https://doi.org/10.1021/acs.accounts.5b00129.
(34) Marwah, P.; Lardy, H. A. Process for Effecting Allylic Oxidation Using Dicarboxylic Acid Imides and Chromium Reagents. US6384251B1, May 7, 2002.
(35) Gondi, V. B.; Loch, J. T. I.; Holman, N. J.; Collier, S. J. Process for the Preparation of 3-Substituted Cannabinoid Compounds, June 8, 2017.
(36) Mechoulam, R.; Lander, N.; University, A.; Zahalka, J. Synthesis of the Individual, Pharmacologically Distinct, Enantiomers of a Tetrahydrocannabinol Derivative. *Tetrahedron: Asymmetry* **1990**, *1* (5), 315–318. https://doi.org/10.1016/S0957-4166(00)86322-3.
(37) Hoffmann, G.; Daniliuc, C. G.; Studer, A. Synthesis of Para (−)-Δ8-THC Triflate as a Building Block for the Preparation of THC Derivatives Bearing Different Side Chains. *Org. Lett.* **2018**. https://doi.org/10.1021/acs.orglett.8b03907.
(38) Dethe, D. H.; Erande, R. D.; Mahapatra, S.; Das, S.; B., V. K. Protecting Group Free Enantiospecific Total Syntheses of Structurally Diverse Natural Products of the Tetrahydrocannabinoid Family. *Chem. Commun.* **2015**, *51* (14), 2871–2873. https://doi.org/10.1039/C4CC08562K.
(39) Hoffmann, G.; Studer, A. Short and Protecting-Group-Free Approach to the (−)-Δ8-THC-Motif: Synthesis of THC-Analogues, (−)-Machaeriol B and (−)-Machaeriol D. *Org. Lett.* **2018**. https://doi.org/10.1021/acs.orglett.8b01005.
(40) Dixon, D. D.; Sethumadhavan, D.; Benneche, T.; Banaag, A. R.; Tius, M. A.; Thakur, G. A.; Bowman, A.; Wood, J. T.; Makriyannis, A. Heteroadamantyl Cannabinoids. *J. Med. Chem.* **2010**, *53* (15), 5656–5666. https://doi.org/10.1021/jm100390h.
(41) Dixon, D. D.; Tius, M. A.; Thakur, G. A.; Zhou, H.; Bowman, A. L.; Shukla, V. G.; Peng, Y.; Makriyannis, A. C3-Heteroaroyl Cannabinoids as Photolabeling Ligands for the CB2 Cannabinoid Receptor. *Bioorganic & Medicinal Chemistry Letters* **2012**, *22* (16), 5322–5325. https://doi.org/10.1016/j.bmcl.2012.06.013.
(42) Bastiaans, H. M. M.; van der Baan, J. L.; Ottenheijm, H. C. J. Flexible and Convergent Total Synthesis of Cyclotheonamide B. *J. Org. Chem.* **1997**, *62* (12), 3880–3889. https://doi.org/10.1021/jo961447m.
(43) Harvey, J. H.; Butler, B. K.; Trauner, D. Functionalized Azobenzenes through Cross-Coupling with Organotrifluoroborates. *Tetrahedron Letters* **2007**, *48* (9), 1661–1664. https://doi.org/10.1016/j.tetlet.2006.12.043.
(44) Potassium Organotrifluoroborates: New Partners in Palladium-Catalysed Cross-Coupling Reactions - Darses - 1999 - European Journal of Organic Chemistry - Wiley Online Library https://onlinelibrary.wiley.com/doi/abs/10.1002/%28SICI%291099-0690%28199908%291999%3A8%3C1875%3A%3AAID-EJOC1875%3E3.0.CO%3B2-W (accessed May 9, 2018).
(45) Molander, G. A.; Petrillo, D. E.; Landzberg, N. R.; Rohanna, J. C.; Biolatto, B. Palladium-Catalyzed Suzuki-Miyaura Reactions of Potassium Aryl- and Heteroaryltrifluoroborates with Aryl- and Heteroaryl Triflates. *Synlett* **2005**, *2005* (11), 1763–1766. https://doi.org/10.1055/s-2005-871544.

(46) Ahmed, Z.; Siiskonen, A.; Virkki, M.; Priimagi, A. Controlling Azobenzene Photoswitching through Combined Ortho-Fluorination and -Amination. *Chem. Commun.* **2017**, *53* (93), 12520–12523. https://doi.org/10.1039/C7CC07308A.
(47) Atwood, B. K.; Wager-Miller, J.; Haskins, C.; Straiker, A.; Mackie, K. Functional Selectivity in CB(2) Cannabinoid Receptor Signaling and Regulation: Implications for the Therapeutic Potential of CB(2) Ligands. *Mol. Pharmacol.* **2012**, *81* (2), 250–263. https://doi.org/10.1124/mol.111.074013.
(48) Felder, C. C.; Joyce, K. E.; Briley, E. M.; Mansouri, J.; Mackie, K.; Blond, O.; Lai, Y.; Ma, A. L.; Mitchell, R. L. Comparison of the Pharmacology and Signal Transduction of the Human Cannabinoid CB1 and CB2 Receptors. *Mol. Pharmacol.* **1995**, *48* (3), 443–450.
(49) Howlett, A. C.; Barth, F.; Bonner, T. I.; Cabral, G.; Casellas, P.; Devane, W. A.; Felder, C. C.; Herkenham, M.; Mackie, K.; Martin, B. R.; Mechoulam, R.; Pertwee, R. G. International Union of Pharmacology. XXVII. Classification of Cannabinoid Receptors. *Pharmacol Rev* **2002**, *54* (2), 161–202.
(50) Demuth, D. G.; Molleman, A. Cannabinoid Signalling. *Life Sciences* **2006**, *78* (6), 549–563. https://doi.org/10.1016/j.lfs.2005.05.055.
(51) Viscomi, M. T.; Oddi, S.; Latini, L.; Pasquariello, N.; Florenzano, F.; Bernardi, G.; Molinari, M.; Maccarrone, M. Selective CB2 Receptor Agonism Protects Central Neurons from Remote Axotomy-Induced Apoptosis through the PI3K/Akt Pathway. *J. Neurosci.* **2009**, *29* (14), 4564–4570. https://doi.org/10.1523/JNEUROSCI.0786-09.2009.
(52) Kurihara, R.; Tohyama, Y.; Matsusaka, S.; Naruse, H.; Kinoshita, E.; Tsujioka, T.; Katsumata, Y.; Yamamura, H. Effects of Peripheral Cannabinoid Receptor Ligands on Motility and Polarization in Neutrophil-like HL60 Cells and Human Neutrophils. *J. Biol. Chem.* **2006**, *281* (18), 12908–12918. https://doi.org/10.1074/jbc.M510871200.
(53) Shoemaker, J. L.; Ruckle, M. B.; Mayeux, P. R.; Prather, P. L. Agonist-Directed Trafficking of Response by Endocannabinoids Acting at CB2 Receptors. *J Pharmacol Exp Ther* **2005**, *315* (2), 828–838. https://doi.org/10.1124/jpet.105.089474.
(54) Rao, G. K.; Kaminski, N. E. Cannabinoid-Mediated Elevation of Intracellular Calcium: A Structure-Activity Relationship. *J Pharmacol Exp Ther* **2006**. https://doi.org/10.1124/jpet.105.100503.
(55) Sugiura, T.; Kondo, S.; Kishimoto, S.; Miyashita, T.; Nakane, S.; Kodaka, T.; Suhara, Y.; Takayama, H.; Waku, K. Evidence That 2-Arachidonoylglycerol but Not N-Palmitoylethanolamine or Anandamide Is the Physiological Ligand for the Cannabinoid CB2 Receptor COMPARISON OF THE AGONISTIC ACTIVITIES OF VARIOUS CANNABINOID RECEPTOR LIGANDS IN HL-60 CELLS. *J. Biol. Chem.* **2000**, *275* (1), 605–612. https://doi.org/10.1074/jbc.275.1.605.
(56) Juan-Picó, P.; Fuentes, E.; Javier Bermúdez-Silva, F.; Javier Díaz-Molina, F.; Ripoll, C.; Rodríguez de Fonseca, F.; Nadal, A. Cannabinoid Receptors Regulate Ca2+ Signals and Insulin Secretion in Pancreatic β-Cell. *Cell Calcium* **2006**, *39* (2), 155–162. https://doi.org/10.1016/j.ceca.2005.10.005.
(57) Tovey, S. C.; Sun, Y.; Taylor, C. W. Rapid Functional Assays of Intracellular Ca 2+ Channels. *Nature Protocols* **2006**, *1* (1), 259–263. https://doi.org/10.1038/nprot.2006.40.
(58) Bleasdale, J. E.; Thakur, N. R.; Gremban, R. S.; Bundy, G. L.; Fitzpatrick, F. A.; Smith, R. J.; Bunting, S. Selective Inhibition of Receptor-Coupled Phospholipase C-Dependent Processes in Human Platelets and Polymorphonuclear Neutrophils. *J Pharmacol Exp Ther* **1990**, *255* (2), 756–768.